

## IMPURITY AND PARTICLE TRANSPORT AND CONTROL IN TFTR

K.W. HILL, V. ARUNASALAM, M.G. BELL, M. BITTER, W.R. BLANCHARD,  
N.L. BRETZ, R. BUDNY, C.E. BUSH<sup>1</sup>, S.A. COHEN, S.K. COMBS<sup>1</sup>,  
S.L. DAVIS, D.L. DIMOCK, H.F. DYLLA, P.C. EFTHIMION,  
L.C. EMERSON<sup>1</sup>, A.C. ENGLAND<sup>1</sup>, H.P. EUBANK, R.J. FONCK,  
E. FREDRICKSON, H.P. FURTH, G. GAMMEL, R.J. GOLDSTON, B. GREK,  
L.R. GRISHAM, G. HAMMETT, R.J. HAWRYLUK, W.W. HEIDBRINK<sup>2</sup>,  
H.W. HENDEL<sup>3</sup>, E. HINNOV, S. HIROE<sup>1</sup>, H. HSUAN, R.A. HULSE,  
K.P. JAEHNIG, D. JASSBY, F.C. JOBES, D.W. JOHNSON, L.C. JOHNSON,  
R. KAITA, R. KAMPERSCHROER, S.M. KAYE, S.J. KILPATRICK,  
R.J. KNIZE, H. KUGEL, P.H. LaMARCHE, B. LeBLANC, C.H. MA<sup>1</sup>,  
D.M. MANOS, D.K. MANSFIELD, R.T. McCANN, M.P. McCARTHY,  
D.C. McCUNE, K. McGUIRE, D.H. McNEILL, D.M. MEADE, S.S. MEDLEY,  
D.R. MIKKELSEN, S.L. MILORA<sup>1</sup>, W. MORRIS<sup>4</sup>, D. MUELLER,  
V. MUKHOVATOV<sup>5</sup>, E.B. NIESCHMIDT<sup>6</sup>, J. O'ROURKE<sup>7</sup>, D.K. OWENS,  
H. PARK, N. POMPHREY, B. PRICHARD, A.T. RAMSEY, M.H. REDI,  
A.L. ROQUEMORE, P.H. RUTHERFORD, N.R. SAUTHOFF, G. SCHILLING,  
J. SCHIVELL, G.L. SCHMIDT, S.D. SCOTT, S. SESNIC, M. SHIMADA<sup>8</sup>,  
J.C. SINNIS, F.J. STAUFFER<sup>9</sup>, J. STRACHAN, B.C. STRATTON, G.D. TAIT,  
G. TAYLOR, J.R. TIMBERLAKE, H.H. TOWNER, M. ULRICKSON,  
V. VERSHKOV<sup>5</sup>, S. VON GOELER, F. WAGNER<sup>10</sup>, R. WIELAND,  
J.B. WILGEN<sup>1</sup>, M. WILLIAMS, K.L. WONG, S. YOSHIKAWA,  
R. YOSHINO<sup>8</sup>, K.M. YOUNG, M.C. ZARNSTORFF, V.S. ZAVERYAEV<sup>5</sup>,  
S.J. ZWEBEN

Princeton Plasma Physics Laboratory,  
Princeton University,  
Princeton, New Jersey,  
United States of America

<sup>1</sup> Oak Ridge National Laboratory, Oak Ridge, TN, USA.

<sup>2</sup> GA Technologies Inc., San Diego, CA, USA.

<sup>3</sup> RCA David Sarnoff Research Centre, Princeton, NJ, USA.

<sup>4</sup> Balliol College, University of Oxford, Oxford, UK.

<sup>5</sup> Kurchatov Institute of Atomic Energy, Moscow, USSR.

<sup>6</sup> EG&G Idaho, Inc., Idaho Falls, ID, USA.

<sup>7</sup> JET Joint Undertaking, Abingdon, Oxfordshire, UK.

<sup>8</sup> JAERI, Naka-machi, Naka-gun, Ibaraki-ken, Japan.

<sup>9</sup> University of Maryland, College Park, MD, USA.

<sup>10</sup> Max-Planck-Institut für Plasmaphysik, Garching, Fed. Rep. Germany.

## Abstract

### IMPURITY AND PARTICLE TRANSPORT AND CONTROL IN TFTR.

Degassing of the TFTR graphite limiter by low density deuterium or helium discharges enables the limiter to pump deuterium, thereby reducing recycling and improving energy confinement in neutral-beam-heated discharges. During a helium degassing sequence the hydrogen influx decreased by a factor of 20. As a consequence of degassing sequences the low density limit in 0.8 MA deuterium discharges decreased from  $1 \times 10^{19} \text{ m}^{-3}$  to  $0.5 \times 10^{19} \text{ m}^{-3}$ , the density decay time dropped from greater than 10 s to 0.15 s, and the recycling coefficient dropped from nearly 1 to less than 0.4.  $Z_{\text{eff}}$  values in 2.2 MA L-mode discharges on the toroidal limiter with neutral-beam-heating power up to 15 MW are between 2 and 3 if the pre-beam plasma has low  $Z_{\text{eff}}$  (high density), but can be as high as 4.5 if the pre-beam plasma has high  $Z_{\text{eff}}$  (low density).  $Z_{\text{eff}}$  values in enhanced confinement shots drop from 7 during the ohmic phase to 3 with neutral beam heating. The radiated power drops from 60-70% of total heating power to 30-35% for beam powers from 10 to 20 MW.

## I. Introduction

Operation of TFTR plasmas on the toroidal graphite limiter at neutral beam powers up to 20 MW has provided new data on plasma-limiter interactions at near reactor temperatures and densities. Discovery of a new regime of enhanced energy confinement in beam-heated discharges [1] has improved prospects for achieving breakeven in TFTR and has provided new insights into the role of edge particle control. Degassing of the limiter to achieve low recycling and documentation of the effect of the degassing on plasma confinement have been a focus of recent experiments [2,3].

A second aspect of plasma-limiter/wall interactions is impurity production and influence of the resulting contamination on the plasma. Plasma impurity levels in L-mode and enhanced confinement discharges with neutral beam powers up to 20 MW are discussed. Impurity transport rates have been inferred by injecting impurities into the plasma and studying the time behavior of their radiation.

## II. Conditioning for Particle and Impurity Control

The large area toroidal limiter [2] required special conditioning techniques to achieve satisfactory plasma operation [4]. Following installation, 130 hours of glow-discharge cleaning (GDC) and 175 hours of pulse-discharge cleaning (PDC) were performed during a six-week period, with the vacuum vessel heated to 150°C. After this conditioning, discharges were severely affected by outgassing of the limiter following a disruption. Additional PDC and a newly developed technique, disruptive discharge cleaning (DDC), were used to heat the limiter surface sufficiently (~1000°C) to effect outgassing of water vapor and hydrocarbons. The DDC consisted of a sequence of tokamak discharges with flat-top currents increasing from 0.6 to 2.5 MA.

The flat-top current was increased progressively by 0.2 MA after a forced disruption at each current did not affect the succeeding discharge. When recovery was easy after a 2.5 MA disruption, ohmic discharges at 2.2 MA had a radiated power fraction less than 50% and  $Z_{\text{eff}} \leq 1.5$  for  $\bar{n}_e > 4 \times 10^{19} \text{ m}^{-3}$ . Following a one-week opening of the vacuum vessel, DDC, in addition to GDC and PDC, was again required to eliminate excessive limiter outgassing caused by a 2.2 MA disruption.

In contrast, only standard GDC and PDC techniques were required to prepare both the vacuum vessel and the movable limiter for high power operation, prior to installation of the toroidal graphite limiter [5]. Following 100-200 discharges, the radiated power fraction and  $Z_{\text{eff}}$  in ohmic fiducial discharges ( $I_p = 1.4 \text{ MA}$ ,  $\bar{n}_e = 2.4 \times 10^{19} \text{ m}^{-3}$ ) dropped to 60 - 70% and 2, respectively.

The initial enhanced confinement neutral-beam-heated discharges were obtained only after degassing the graphite limiter by several tens of low density helium and deuterium discharges. Evidently, desorption of deuterium from the normally saturated near-surface region of the graphite enabled the limiter to retain

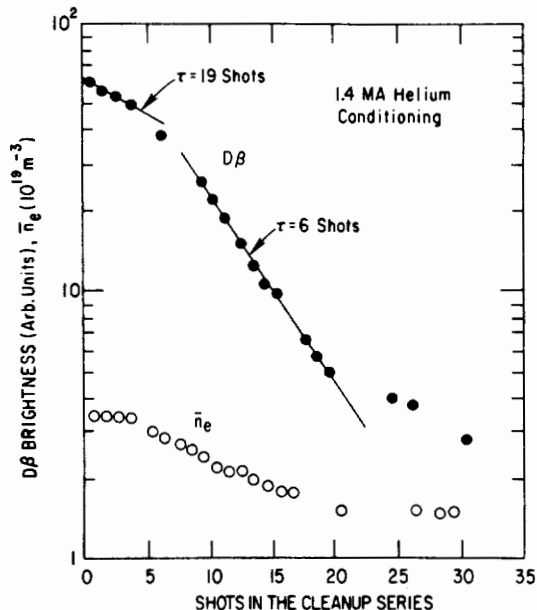


FIG. 1.  $D\beta$  emission intensity and line-averaged electron density during a sequence of low density 1.4 MA helium limiter degassing discharges. A decrease in the deuterium influx of a factor of 20 indicates depletion of deuterium from the surface and near surface regions of the limiter.

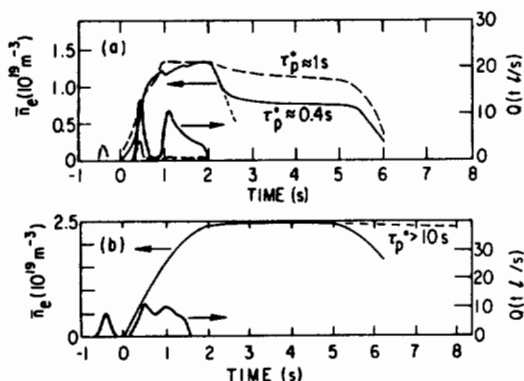


FIG. 2. Line-averaged electron density and gas fueling rate as a function of time during fiducial shots on: (a) a well conditioned limiter (solid line) and a deconditioned limiter (dashed line), and (b) an unconditioned limiter.

incident hydrogen efficiently and substantially reduced recycling. In combination with intense central fueling by neutral beam injection, the lower recycling produced a more peaked density profile. During normal enhanced-confinement operation, daily sequences of about 10 degassing shots were used to keep plasma performance optimized. About 20-30 degassing shots were required to recover from gas loading caused by pellet-fueled [6] or detached plasmas [7].

The hydrogen degassing by a series of 1.4 MA helium conditioning discharges on the toroidal limiter is illustrated by Fig. 1. The brightness of the deuterium D $\beta$  line ( $n = 4-2$  transition), which is a measure of the deuterium influx into the plasma, decreased by a factor of 20 during this sequence. The minimum achievable line-averaged electron density also decreased by a factor of two, as shown, and oxygen radiation decreased by an order of magnitude. This suggests that conditioning discharges also remove oxygen, possibly in the form of water vapor or CO. The intensity of carbon radiation changed little during the sequence.

Two important consequences of the limiter degassing are a smaller low-density limit and a shorter density-decay time, constant or effective particle confinement time  $\tau_p^*$ , indicated by faster density pumpout. Both effects are illustrated in Fig. 2a, which shows the time evolution of the central-chord line-averaged electron density and the gas input rate for 2 shots, one before and one after a 25-shot 0.8 MA deuterium degassing sequence. In contrast, a large value of  $\tau_p^*$  ( $> 10$  s) characterized the toroidal limiter before conditioning sequences were begun (Fig. 2b). In these fiducial discharges the gas feed is controlled by feedback to produce a preselected density at  $t = 2$  s

and is then shut off. Figure 2a depicts 0.8 MA discharges programmed to  $\bar{n}_e = 1.3 \times 10^{19} \text{ m}^{-3}$ , whereas Fig. 2b is a 1.4 MA discharge programmed to  $\bar{n}_e = 2.4 \times 10^{19} \text{ m}^{-3}$ . The density decays exponentially to a baseline which is determined by recycling. The density decay time is determined by the intercept of the dashed lines, which characterize the initial decay rate, with the minimum density baseline.

Decay time constants as small as 0.15 s were obtained after applying helium degassing sequences frequently over a 1000-shot interval. The sequences were interspersed with series of neutral-beam-heated shots to test the effectiveness of conditioning on improving beam fueling and energy confinement. During this period the minimum line-averaged density achievable in 0.8 MA deuterium discharges decreased from  $0.9 \times 10^{19} \text{ m}^{-3}$  to  $0.55 \times 10^{19} \text{ m}^{-3}$ .

The recycling coefficient in ohmic discharges,  $R$ , is determined from  $\tau_p$  and the particle confinement time,  $\tau_p$ , by the equation

$$\tau_p^* = \frac{\tau_p}{1-R} \quad (1)$$

$\tau_p$  as measured by the absolute intensity of the  $\text{D}\alpha$  emission is on the order of 0.1 s. Thus, the fastest density decay times, 0.15 - 0.3 s, correspond to a recycling coefficient of  $R < 0.5$ .

Helium discharges with  $I_p = 1.4$  and 1.8 MA were more effective in degassing the limiter than were 0.8 MA deuterium discharges. A few shots in deuterium are required to expel the residual helium, but the succeeding discharges have lower densities than can be achieved following conditioning by deuterium discharges. There are indications that higher current helium discharges are more effective than lower current discharges.

The limiter degassing effect is easily reversed by exposure to higher density deuterium plasmas. An estimated 100 torr-liters ( $7.1 \times 10^{21}$  atoms) of total gas input over a few discharges will increase the recycling coefficient to approximately 1. Deuterium gas-fueled 0.8 MA ohmic discharges with  $\bar{n}_e$  as low as  $1.2 \times 10^{19} \text{ m}^{-3}$  can produce a noticeable degradation.

The limiter degassing is believed to result from desorption of hydrogen from the graphite by energetic carbon and helium ion bombardment. Graphite can absorb hydrogen up to a H/C ratio of 0.4 at room temperature. Spectroscopic measurements and  $Z_{\text{eff}}$  values of six to seven show that the carbon density in degassing discharges is high. Recent measurements by Wampler *et al.* [8] show that bombardment of saturated graphite by carbon, helium, or hydrogen ions with energies of 3, 0.6 and 0.3 keV, respectively (consistent with the edge electron temperature and sheath potential in these discharges) removes 5, 2 and 1 hydrogen atoms per incident ion, the latter case resulting in replacement, with

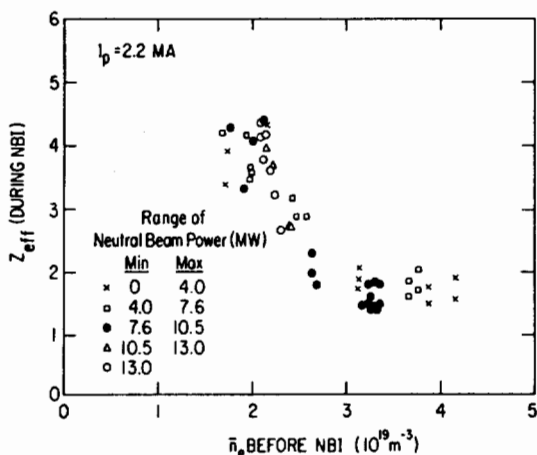


FIG. 3.  $Z_{\text{eff}}$  during neutral-beam injection as a function of electron density before injection, sorted by ranges of neutral-beam power. The values are near the pre-NBI  $Z_{\text{eff}}$  values, but somewhat reduced owing to neutral-beam fueling.

no net removal of hydrogenic species. Also, the yields for sputtering carbon atoms from graphite are 0.5, 0.09 and 0.025 atoms/ion for these three ions. Thus the degassing process is aided by the low density, high edge temperature, and the resultant high levels of carbon impurities.

### III. Plasma Impurity Concentrations in the Standard Regime

Impurity concentrations and  $Z_{\text{eff}}$  have been measured by x-ray and vacuum ultraviolet spectroscopy and visible bremsstrahlung; the total radiated power has been measured by bolometer arrays. These measurements have documented the effectiveness of impurity control techniques, provided quantitative data on the variation of impurities over a wide range of plasma parameters, and provided additional information on impurity sources and impurity production mechanisms [9-11].

The impurity situation in ohmically heated TFTR discharges is discussed in Refs [9-11]. Impurity concentrations were low ( $Z_{\text{eff}} = 1.2$ ) at high density, but were significant ( $Z_{\text{eff}} = 5-6$ ) at the low-density limit for 2.2 MA plasmas on either the movable or toroidal limiter. Discharges on the toroidal limiter had lower  $Z_{\text{eff}}$  at intermediate densities than those on the movable limiter [12]. The low- $Z$  impurities, carbon and oxygen, ranged from about 10% of electron density (at low  $n_e$ ) to 1% (high  $n_e$ ) and were the dominant contributors to  $Z_{\text{eff}}$  and radiated power. The ratio of carbon to oxygen was about 10 at low density and 1 at high density. Oxygen increased with density and dominated the radiated power at the high density limit [11]. Metals (Cr, Fe, Ni) were generally negligible contributors to  $Z_{\text{eff}}$  and radiated power.

Impurity behavior in 2.2 MA neutral-beam-heated plasmas on the movable limiter with beam power up to 5.6 MW has been discussed previously [11]. In a beam-power scan at constant final density ( $\bar{n}_e = 4.5 \times 10^{19} \text{ m}^{-3}$ ),  $Z_{\text{eff}}$  near the end of the 0.5 s heating pulse increased from less than 2 to about 3 as beam power increased to 5.6 MW. During a discharge, metal and carbon densities remained constant from the pre-beam to the beam-heated phase. Thus, higher  $Z_{\text{eff}}$  at higher power results mainly from the lower pre-beam density (and therefore higher  $Z_{\text{eff}}$ ) required to keep the final density constant. The fraction of total input power radiated decreased from about 50% in the ohmic phase to 30% at a beam power greater than 3 MW.

$Z_{\text{eff}}$  values in 2.2 MA, L-mode beam-power scans on the toroidal limiter also correlated much more strongly with the electron density in the pre-beam ohmic heating phase of discharges than with beam power or with density at the end of injection (Fig. 3). The data, measured by x-ray pulse-height analysis, have been sorted according to ranges of beam power. Low  $Z_{\text{eff}}$  values ( $\leq 2$ ) are achieved during neutral-beam injection (NBI) if the ohmic target plasma is clean ( $\bar{n}_e > 3 \times 10^{19} \text{ m}^{-3}$ ), while higher  $Z_{\text{eff}}$  values during NBI occur if the ohmic plasma is dirty (low density). The trend is similar to that of pre-beam  $Z_{\text{eff}}$  versus  $\bar{n}_e$ , although shifted slightly lower, due to dilution of impurities by neutral-beam fueling.  $Z_{\text{eff}}$  values measured from visible bremsstrahlung emission were on the average 15% higher than the values from pulse-height analysis for most of these shots.

The radiated-power fraction in these L-mode discharges on the toroidal limiter decreased to about 20% for neutral beam powers greater than 10 MW.

#### IV. Impurity Concentrations in Enhanced Confinement Plasmas

The pre-injection target plasmas in enhanced confinement discharges are carbon dominated, with a total  $Z_{\text{eff}}$  of six to eight and a  $Z_{\text{eff}}$  contribution of 0.3 - 1.5 from metals. The carbon concentration is about 15% of the electron density. The deuteron fraction is estimated to be between 10% and 20%, based on the increase in neutron emission following a small gas puff. During neutral beam injection,  $Z_{\text{eff}}$  from visible bremsstrahlung drops to 2-4 (Fig. 4 and earlier data). The earliest enhanced confinement plasmas had  $Z_{\text{eff}}$  values of 2-3 during the beam-heating phase, with a negligible contribution from metals. Subsequent limiter conditioning and plasma operation, spanning 1000 discharges over a period of five weeks, increased the metal levels by a factor of 10, presumably by depositing metals removed from inconel hardware near the limiter onto the graphite surface.

During neutral beam heating, the fueling by the beam neutrals increases the deuteron fraction to 50-60% of electron density and decreases the carbon fraction to 5-8%. The fraction

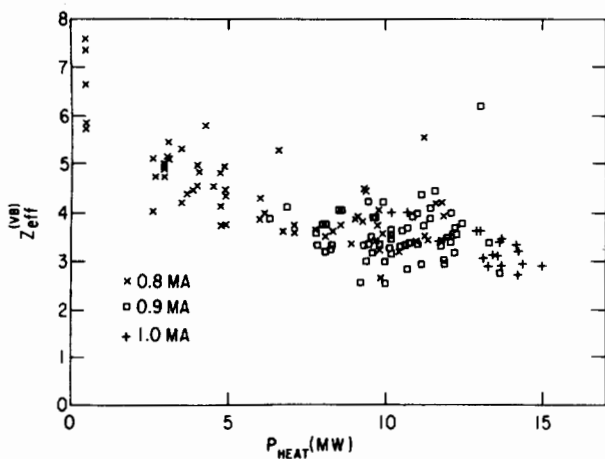


FIG. 4.  $Z_{eff}$  as a function of total heating power in enhanced confinement discharges.

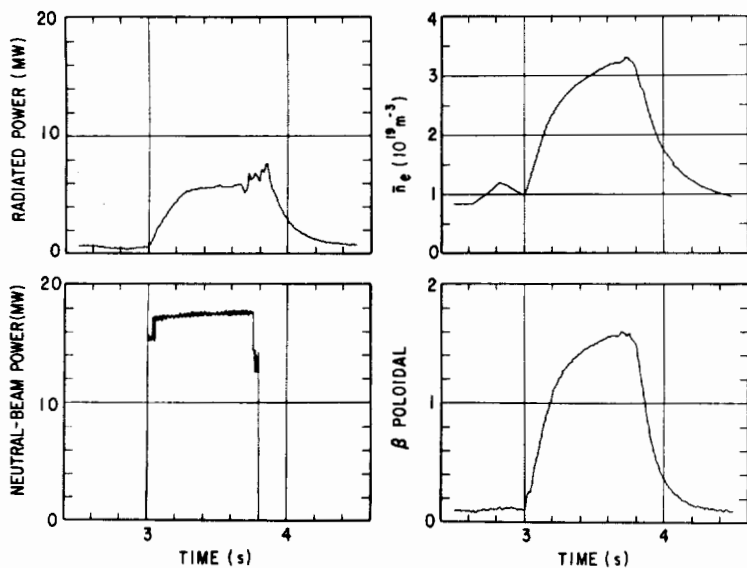


FIG. 5. Total radiated power, line-averaged electron density, neutral-beam power and poloidal beta, as a function of time during a 1.1 MA enhanced confinement discharge with a 0.7 s beam-heating pulse.



of total heating power radiated decreases from 60-70% during the ohmic phase to about 30% for beam powers greater than 10 MW. For longer pulse (0.7 s) beams the total radiated power saturates while electron density and  $\beta_p$  are still rising, as shown in Fig. 5.

The impurity transport during beam heating in enhanced confinement discharges appears to be similar to that during the ohmic phase. Transport rates were inferred from the time evolution of vacuum-ultraviolet lines emitted by germanium injected into the plasma by laser ablation. Comparison of these intensities with numerical impurity transport code predictions [13] yielded a diffusion coefficient (assumed to be radially constant) and convective velocity at the limiter radius of 0.65  $m^2/s$  and 0 - 0.1 m/s, respectively, in the ohmic phase, and 0.75  $m^2/s$  and 0.1 - 0.2 m/s, respectively, during neutral beam injection. The uncertainty in the convective velocity is a factor of 2. The impurity confinement time in both cases was approximately 0.25 s.

## V. Summary and Conclusions

A disruptive discharge cleaning procedure, in addition to glow- and pulsed-discharge cleaning, was found necessary following atmospheric exposure to remove water vapor from the large-area graphite toroidal limiter and permit satisfactory plasma operation.

Low density deuterium or helium discharges were found to be effective in degassing the limiter, allowing it to pump hydrogen and, thus, reduce recycling and permit improved confinement in neutral-beam-heated discharges. High carbon concentrations and  $Z_{eff}$  appear to aid degassing by causing high edge temperatures and leading to desorption of deuterium by energetic carbon ion bombardment.

Relatively low  $Z_{eff}$  values (about 2) were attained in high density L-mode discharges on the toroidal limiter, with beam powers up to 10 MW, and values of 2.5 - 3 were found at beam powers up to 15 MW. The trends suggest, however, that the purity of the pre-beam target plasma is a more important determinant of impurity concentrations during NBI than is beam power or final density.

Enhanced confinement plasmas are characterized by a  $Z_{eff}$  of six to seven before neutral beam injection and two to four during injection.  $Z_{eff}$  decreases with beam power, presumably due to the dominance of beam fueling in these plasmas.

There is no evidence of significant changes in impurity transport between ohmic and enhanced confinement discharges.

### Acknowledgments

We are grateful to J.R. Thompson and D. Grove for their support. This work was supported by US DOE Contract No. DE-AC02-76-CH03073. The ORNL participants were also supported by US DOE Contract No. DE-AC05-84OR21400 with Martin Marietta Energy Systems, Inc.

### REFERENCES

- [1] STRACHAN, J.D., et al., submitted to Phys. Rev. Lett.
- [2] HAWRYLUK, R.J., et al., paper IAEA-CN-47/A-I-3, these Proceedings, Vol. 1.
- [3] GOLDSTON, R.J., et al., Paper IAEA-CN-47/A-I-4, these Proceedings, Vol. 1.
- [4] DYLLA, H.F., et al., submitted to Nucl. Fusion.
- [5] LA MARCHE, P.H., et al., J. Nucl. Mater. **145&146** (1987).
- [6] MILORA, S.L., et al., paper IAEA-CN-47/A-III-4, these Proceedings, Vol. 1.
- [7] STRACHAN, J., et al., in Controlled Fusion and Plasma Physics (Proc. 12th Europ. Conf. Budapest, 1985), Pt. I, European Physical Society (1985) 339.
- [8] WAMPLER, W., DOYLE, B., BRYCE, D., submitted for publication.
- [9] HILL, K.W., et al., Nucl. Fusion **26** (1986) 1131.
- [10] DYLLA, H.F., et al., J. Nucl. Mater. **145&146** (1987).
- [11] STRATTON, B.C., et al., submitted to Nucl. Fusion.
- [12] BELL, M.G., et al., Plasma Phys. Controll. Fusion **28** (1986) 1329.
- [13] STRATTON, B.C., et al., J. Nucl. Mater. **145&146** (1987).

### DISCUSSION

F.C. SCHÜLLER: It is normally accepted that the high density limit for disruptions decreases with increasing  $Z_{\text{eff}}$ . You quote for the high density Ohmic discharges a  $Z_{\text{eff}}$  which is considerably lower than that in JET, whilst your density limit is lower. Do you get 100% radiation just before disruption?

K.W. HILL: In Ohmic discharges, the high density limit in TFTR is higher than that in JET; however, the Murakami parameters are comparable. The good agreement in the  $Z_{\text{eff}}$  determination between the various diagnostics, as described in the paper, gives us confidence in our low values of  $Z_{\text{eff}}$  at high density. At the density limit the power radiated is about 100%. The question then arises whether the usual Murakami/Hugill parameter coupled with  $Z_{\text{eff}}$  determines the operating boundary accurately. Perhaps the operational limit depends, in addition, on plasma elongation and on the toroidal field — in a manner other than that implied by the relationship given by the Murakami/Hugill parameter.